M. Tech (Power Electronics and Systems)

Design, Analysis and Control of LLC Resonant Converter

DISSERTATION/THESIS

SUBMITTED IN PARTIAL FULFILLMENT OF THE REQUIREMENTS
FOR THE AWARD OF THE DEGREE
OF

MASTER OF TECHNOLOGY
IN
POWER ELECTRONICS & SYSTEMS

Submitted by:

KUMAR SAGAR

2K22/PES/09

Under the supervision of

PROF. MINI SREEJETH
(Professor, EED, DTU)

Mr. GAURAV KAUSHIK
(Assistant Professor, EED, DTU)

DEPARTMENT OF ELECTRICAL ENGINEERING
DELHI TECHNOLOGICAL UNIVERSITY
(Formerly Delhi College of Engineering) Bawana Road, Delhi-110042

MAY2024

2024

DEPARTMENT OF ELECTRICAL ENGINEERING

DELHI TECHNOLOGICAL UNIVERSITY

(Formerly Delhi College of Engineering)

Bawana Road, Delhi-110042

CANDIDATE'S DECLARATION

I, **KUMAR SAGAR,** Roll No. 2K22/PES/09 student of M. Tech (Power Electronics & Systems), hereby declare that the project Dissertation titled **"Design, Analysis and Control of LLC Resonant Converter"** which is submitted by me to the Department of Electrical Engineering Department, Delhi Technological University, Delhi in partial fulfillment of the requirement for the award of the degree of Master of Technology, is original and not copied from any source without proper citation. This work has not previously submitted for the award of any Degree, Diploma.

Place: Delhi **(Kumar Sagar)**

Date: 31/05/2024

CERTIFICATE

I hereby certify that the project Dissertation titled **"Design, Analysis and Control of LLC Resonant Converter"** which is submitted by Kumar Sagar, Roll No. 2K22/PES/09, Department of Electrical Engineering, Delhi Technological University, Delhi in partial fulfilment of the requirement for the award of the degree of Master of Technology ,is a record of the project work carried out by the student under my supervision. To the best of my knowledge this work has not been submitted in part or full for any Degree or Diploma to this University or elsewhere.

Place: Delhi

Date: 31.05.2024

PROF. MINI SREEJETH

(SUPERVISOR)

Mr. GAURAV KAUSHIK

(CO-SUPERVISOR)

ACKNOWLEDGEMENT

I would like to express my gratitude towards all the people who have contributed their precious time and effort to help me without whom it would not have been possible for me tounderstand and complete the project.

I would like to thank **Dr. Mini Sreejeth** (Professor, Department of Electrical Engineering, DTU, Delhi) and **Mr. Gaurav Kaushik** (Assistant Professor, Department of Electrical Engineering, DTU, Delhi) my Project guide and co-guide respectively, for supporting, motivating and encouraging me throughout the period of this work was carried out. His readiness for consultation always, his educative comments, his concern and assistance even with practical things have been invaluable. I would also like to thank the Centre of Excellence for Electric Vehicles and Related Technologies, Delhi Technological University for providing necessary facilities for performing my research work.

Finally, I must express my very profound gratitude to my parents, seniors and to my friends for providing me with unfailing support and continuous encouragement throughout the research work.

Date: 31/05/2024

kumar Sagar

M. Tech (Power Electronics & Systems)

Roll No. 2K22/PES/09

ABSTRACT

The Ongoing demand for electric vehicles (EVs) has intensified research efforts towards enhancing the efficiency and effectiveness of charging systems. Among various topologies, LLC resonant converters have been emerged as a promising solution having to their high efficiency, reduced electromagnetic interference, and inherent soft-switching characteristics.

This abstract provides a comprehensive review of recent advancements in LLC resonant converters specifically tailored for EV charging applications. The abstract begins by explaining the fundamental principles underlying LLC resonant converters, emphasizing their unique advantages over conventional converter topologies. Subsequently, it highlights the key challenges associated with EV charging, such as high-power demands, grid integration issues, and charging infrastructure limitations.

TABLE OF CONTENTS

LIST OF FIGURES

LIST OF TABLES

LIST OF ABBREVIATIONS

LLC	Inductor Inductor Capacitor
ZVS	Zero Voltage Switching
ZCS	Zero current Switching
CC	Constant Current
CV	Constant Voltage
PI	Proportional Integrator
EV	Electric Vehicle
UPF	Unity Power Factor
SRC	Series resonant converter
PRC	Parallel resonant converter
DBR	Diode Bridge Rectifier
EMI	Electro Magnetic Interference
F_S	Switching frequency
F_R	Resonating frequency
FHA	First harmonic approximation
PFM	Pulse frequency modulation

CHAPTER 1
INTRODUCTION

1.1 Overview

There are two types of DC-DC converters: resonant converters and pulse-width-modulation (PWM) converters. Since the majority of applications require a regulated voltage output, the control system includes a feedback loop to stablish the output voltage. Small-signal equivalent circuit models are essential for the best possible design.

The most basic type of resonant converter is the series resonant converter (SRC). The state-space averaging technique is not effective to resonant converters. The explanation is because while dc components predominate in state variables for PWM converters, some state variables for resonant converters include large switching frequency components and their harmonics instead of dc components. The switching frequency interacts with the natural resonant frequency because of the intense oscillatory character of resonant states. This leads to a strange phenomenon known as the beat frequency dynamics, in which a pair of double poles situated at the beat frequency control the high-frequency response.

By using phase-shift modulation as an additional control parameter, the necessary range of switching frequencies to obtain the same voltage conversion ratio is reduced. However, it is necessary to have a precise calculation of the state variables under all operating situations in order to effectively evaluate the trade-off between power density and efficiency during the design process. For instance, I suggest utilising phase-shift modulation while employing the first harmonic approximation (FHA) to construct the converter. When a converter with a low-quality factor (Q) operates in discontinuous conduction mode (DCM) and uses phase-shift modulation, an FHA- based technique becomes highly incorrect.

1.2 THESIS MOTIVATION:

In the current scenario of EV market, availability of off-board EV charger at certain distance is the major concern. This will reduce the range anxiety among the users and will rise the sales of EVs and make growth of EV market in India stable. That's why this research area was selected to work upon and to add some contribution in the power converters for off- board EV charging.

1.3 Thesis organization:

This Thesis consists of complete design analysis and voltage control of the LLC resonant converter under different load. The outline of this this thesis is as follows:

Chapter 1: This chapter provides the reader with an introduction to the LLC Resonant converter its importance in the power electronics. In the chapter we have discuss about the frequency modulation of LLC converter.

Chapter 2: In this chapter we have discussed about the Full bridge LLC resonant converter. This chapter provides the difference between the Full bridge and half bridge of switching.

Chapter 3: In this chapter we have design a Full bridge LLC resonant circuit for 3.3KW output power and its magnetics.

Chapter 4: In this chapter we have done the voltage control of Full bridge LLC resonant converter at different resistive and DC motor load.

Chapter 5: This chapter validates the results of the systems at various load conditions, and also discussed the simulation results.

Chapter 6: This chapter summarize the Design analysis and control of LLC resonant converter and propose some future work.

1.4 Literature Review:

[1] This Paper examines the application of dual closed loop control to improve the efficiency of LLC resonant converters in the charging of electric vehicle (EV) batteries. This method employs dual feedback loops to accurately control voltage and current, hence enhancing efficiency, stability, and dynamic response. Their work focuses on tackling crucial obstacles in electric vehicle charging, such as ensuring optimal power conversion and consistent functioning under fluctuating load conditions. The study provides useful insights for enhancing the efficiency of EV charging systems and recommends further investigation into sophisticated control strategies and materials to drive future advancements.

[2] This paper discusses the difficulties associated with maintaining optimal efficiency in converters when operating at varying voltage levels. The hybrid-secondary-rectifier (HSR) is implemented in dual half-bridge LLC resonant converters to improve performance. This is particularly important for applications such as renewable energy systems and battery charging. The study enhances the field by suggesting sophisticated control algorithms to optimise converter performance in the presence of changing load conditions.

[3] This Paper work aims to optimise high-efficiency Full-bridge LLC resonant converters, in line with current research trends that aim to enhance efficiency by employing sophisticated design and control methodologies. Their research expands upon prior investigations that highlight the significance of accurate modelling, sophisticated semiconductor materials such as GaN, and inventive control techniques to improve the efficiency and dependability of converters in diverse fields such as renewable energy and electric automobiles.

[4] This paper study examines the efficiency of LLC resonant converters employing interleaving techniques while maintaining a consistent switching frequency. Interleaving decreases the fluctuation in electric current, increases the effectiveness, and promotes the control of heat. The paper examines the differences between open loop control, which is less complex but lacks adaptability, and closed loop control, which dynamically adjusts to enhance stability and performance.

[5] This paper discusses the necessity of achieving efficient and dependable power conversion in renewable energy systems. The researchers concentrate on the particular

demands of PV motor drives and utilise innovative modelling methods to enhance the efficiency and performance of converter designs in different solar situations. This research provides evidence to promote the advancement of sustainable energy solutions and proposes potential strategies for improving the incorporation of LLC resonant converters in photovoltaic (PV) applications.

[8] This work provides a thorough analysis of power loss mechanisms in full-bridge LLC resonant converters, with a focus on their exceptional efficiency and minimal electromagnetic interference resulting from zero-voltage and zero-current switching. The text compares the full-bridge and half-bridge topologies, highlighting the improved performance of the former in higher power applications. The study also emphasises several design and optimisation methodologies that are focused on maximising converter efficiency, such as precise modelling and methods for predicting losses.

[18] This work introduces a sophisticated digital control method that is specifically tailored for rapid charging of electric vehicles (EVs). The system employs two interconnected control loops to regulate voltage and current. This simplifies the complex seventh-order model of the LLC converter to a first-order approximation at resonance, resulting in improved performance in strongly underdamped situations. Incorporating a look-up table (LUT) into the feed-forward path effectively deals with non-linearities, guaranteeing resilient and responsive performance over the whole operational range. The effectiveness and efficiency of the suggested technique are confirmed through rigorous testing using both models and experiments on a 15 kW prototype, showcasing its practical applicability. The literature review emphasises the significance of these converters in electric vehicle (EV) charging because of their high efficiency and power density. It also places this study within the context of broader efforts to improve control strategies and address system non-linearities

This paper investigates the incorporation of LLC resonant converters into the Constant Current Constant Voltage (CCCV) topology to improve the efficiency and dependability of battery charging. LLC resonant converters are renowned for their exceptional efficiency and minimal electromagnetic interference (EMI), whilst the CCCV design is highly successful in safeguarding battery health and optimising charge durations. The study centres on the meticulous design and optimisation of the

components in the resonant tank, utilising sophisticated control algorithms to enhance performance parameters such as efficiency, thermal management, and charging speed. This research is highly pertinent to the fields of electric vehicles, renewable energy storage, and portable electronics. It provides valuable insights for the advancement of battery charging systems.

CHAPTER 2
ANALYSIS OF FULL BRIDGE LLC CONVERTER

2.1 Overview

LLC resonant converters have become an important discussion in power electronics because they have the features of Higher efficiency, higher power density, Low EMI for design of power supply. Resonant power converters i.e LLC half-bridge configuration and LLC full bridge configuration have advantages of higher switching frequencies and lower switching losses. Design of LLC resonant converter require more effort and challenges than PWM converters because for power conversion the LLC resonant performs power frequency modulation instead of pulse-width modulation.

2.2 Brief discussion on Resonant Converters

There are many resonant-converter topologies and they all function in the same way. Their basic operation involves using power switches to generate a square pulse of voltage or current, which is then applied to a resonant circuit. The energy then transferred to the output to supply power. Among the various types of resonant converters, the series resonant converter (SRC) and the parallel resonant converter (PRC) are the most common. Both converter operates by changing the frequency of voltage to change the impedance.

2.2.1 Series resonant converter:

The SRC regulates its output voltage by varying the frequency of the input voltage, which changes the impedance of the resonant circuit. This circuit, in turn, acts as a voltage divider between the input voltage and the load. DC gain of SRC is always less than or equal to one, due to which it is difficult to regulate the output under light-load conditions. At light loads, the load impedance becomes very large so extremely high frequencies is required to maintain output regulation.

$$f_o = \frac{1}{2\pi\sqrt{L_r C_r}}$$

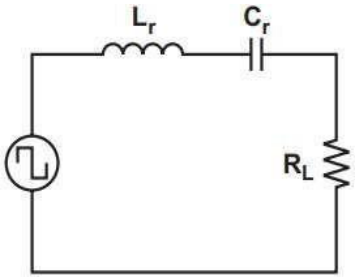

Fig 2.1: Series Resonant Converter

2.2.2 Parallel resonant converter:

In the Parallel resonant converter, the load is connected in parallel with the resonant circuit, which results in large circulating currents. Due to the disadvantages of large circulating currents Parallel resonant converter is not use for applications with high power density because it can lead to unstable output.

$$f_p = \frac{1}{2\pi\sqrt{(L_r + L_m)C_r}}$$

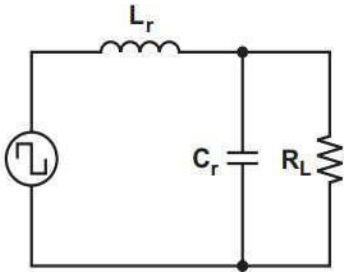

Fig 2.2: Parallel resonant converter

2.2.3 LLC Resonant Converter:

To address these limitations, combination of series resonant converter and Parallel resonant converter is formed. This converter has the advantages of both of series-parallel resonant converter. The structure of this Converter has two inductors and one capacitor.

The advantages of LLC resonant converter compared to resonant converters is that with small deviation in switching frequency LLC resonant converter can regulates wide variation of Line and Load. Additionally, LLC is capable of achieving zero voltage switching (ZVS) throughout its range.

2.3 Full Bridge LLC resonant converter:

Resonant tanks are made up of inductors and capacitors that oscillate at a specific frequency called the resonant frequency. In An LLC converter there are 4 blocks: 1) Power switches, 2) resonant tank, 3) Transformer, and 4) Diode rectifier

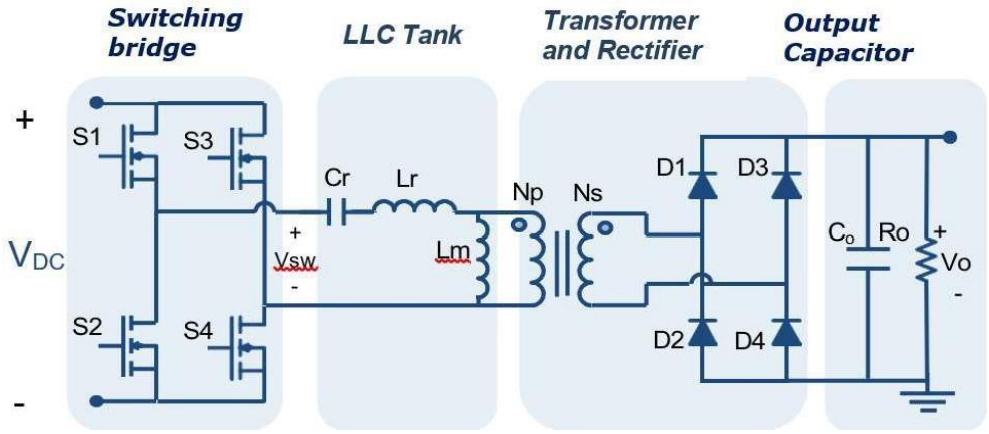

Fig. 2.3 LLC resonant converter

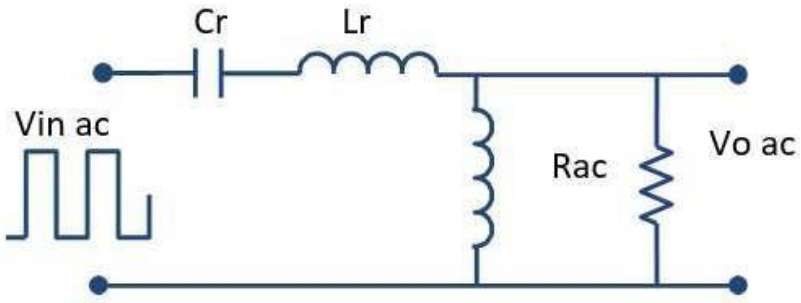

Fig. 2.4 Equivalent Resonant circuit

First, the MOSFET power switches transform the input DC voltage into a high-frequency square wave. That high-frequency square wave fed to the resonant tank. Resonant tank filters out the higher order harmonics and produces the fundamental sine wave. Now the fundamental sine wave will transfer to secondary through

transformer, where the secondary voltage will be adjusted accordingly to transformer ratio. At output side Diode rectifier converts voltage into stable output. The power switches can have two topologies full-bridge or half-bridge.

2.4 Operational principle of Full bridge LLC converter:

230V AC grid supply is given to Full bridge rectifier to get DC voltage. Output of rectifier is fed to Boost PFC converter through which we get 400V DC voltage at good power factor. This 400V DC voltage is fed to LLC converter. This 400V supply voltage is then converted into high frequency square wave with the help of power MOSFETs switches. In LLC full bridge converter switches are operated in pairs (S1, S4) & (S2, S3). In LLC converter duty cycle does not vary but fix and typically equal to 50%. In LLC, switching frequency varies in order to regulate the output voltage and operate near resonant frequency.

There will be only two types of operations:

A. Power delivery operation

B. Freewheeling operation

2.4.1 Power delivery operation (S1, S4 are ON)

Power delivery operation will happen in two cases when resonant tank gets positive half cycle of voltage or negative half cycle of voltage that comes after power MOSFETs switching. During positive half cycle at resonant tank Switches pair (S1, S4) gets ON and switches pair (S2, S3) are OFF. When resonant tank excited with positive voltage then current also resonant in positive direction in the first half of switching cycle. The positive mode of operation is shown in Fig 2.5. As Current flows through the resonant tank it stores the energy. With the help of transformer, the power will deliver to secondary side of rectifier. In Secondary side Diode (D1, D4) gets conducted and input power will get delivered to output side. At output Positive power will get delivered.

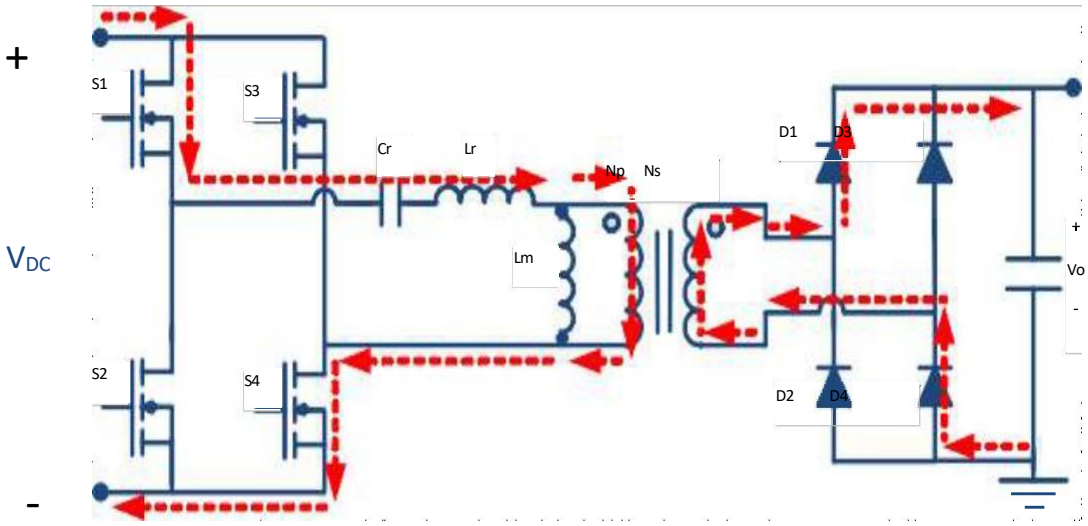

Fig 2.5 Power delivery operation when (S1, S4) is ON

2.4.2 Freewheeling operation (Dead time):

During Freewheeling operation No power delivery will happen to secondary side. This operation is known as freewheeling because the energy got stored during power delivery operation in resonant tank will discharge through the body diodes of MOSFETs. Freewheeling operation will happen during dead time. During dead time both the switching pair will be OFF. Dead time is provided between two switching cycle so that voltages formed across switches will discharge and it will help Zero voltage switching (ZVS). In this mode the charge formed in the resonant tank will discharge through the body diode of the other switches pair (S2, S3). At Dead time Resonant inductor current will be same as magnetising inductor current. In this mode No power will be transfer to the secondary side as shown in fig 2.6.

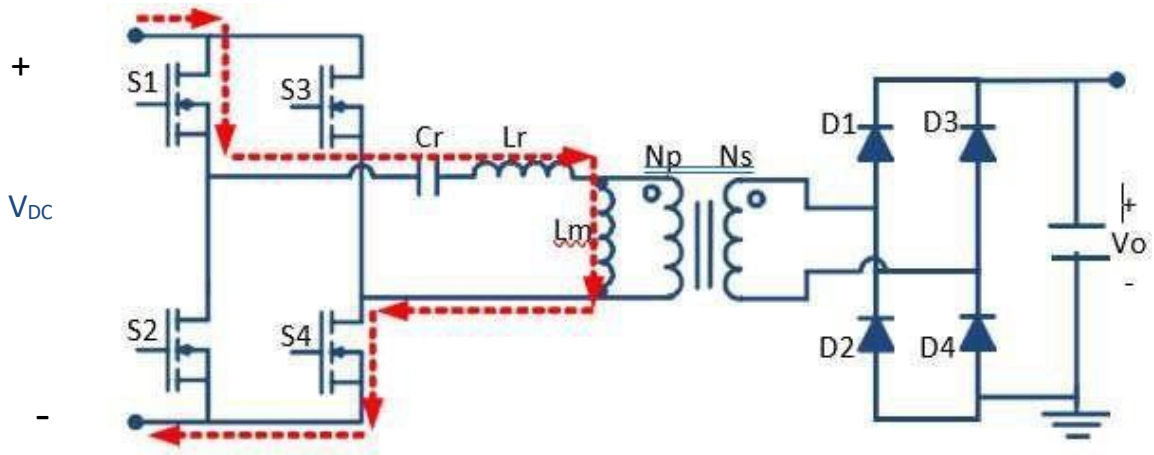

Fig 2.6 Freewheeling operation after (S1, S4) OFF

2.4.3 Power delivery operation (S2, S3 are ON):

After dead time, Resonant tank will get excited with negative half cycle which comes after power MOSFETs switching. In negative half cycle at resonant tank switches pair (S2, S3) gets ON and switches pair (S1, S4) are OFF. When resonant tank excited with Negative voltage then current also resonant in negative direction in the second half of switching cycle as shown in fig 2.6. Like Positive voltage cycle, resonant tank will store energy and power will be delivered to secondary side through transformer. In Secondary side Diode (D2, D3) gets conducted and input power will get delivered to output side. At output Positive power will get delivered.

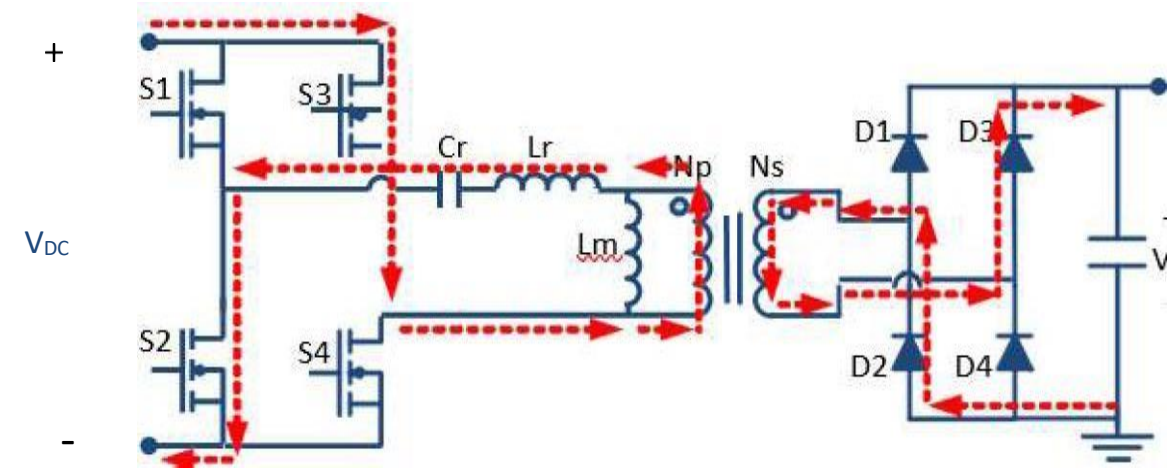

Fig 2.7 Power delivery operation when (S2, S3) is ON

2.4.4 Freewheeling operation (Dead time):

Again, after second cycle both switching pair will gets OFF. During Freewheeling mode resonant tank will discharge through other switches pair (S1, S4) diodes as shown in fig 2.8. No power will deliver during this mode.

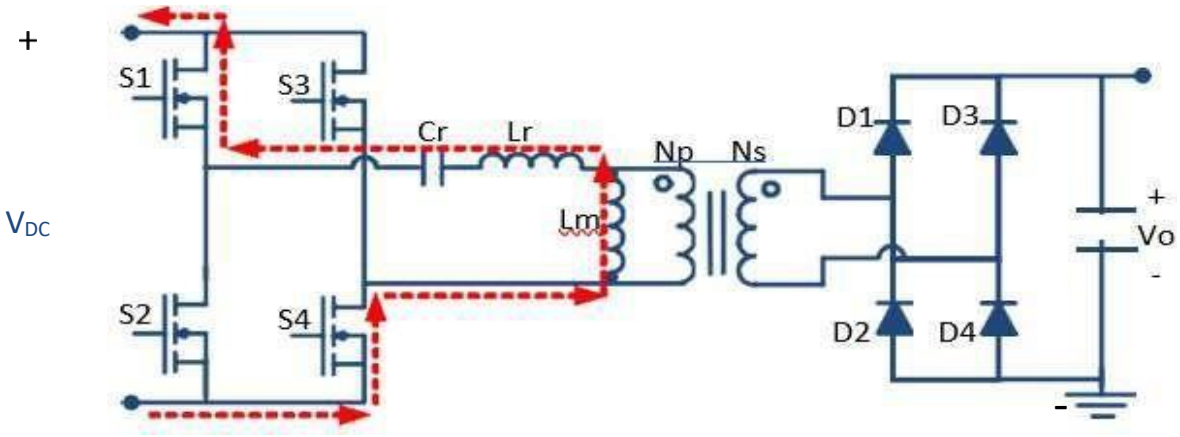

Fig 2.8 Freewheeling operation after (S2, S3) OFF

2.5 Modes of operations:

I. At Resonant frequency (fs=fr.).

II. Below Resonant frequency (fs< fr).

III. Above Resonant frequency (fs>fr).

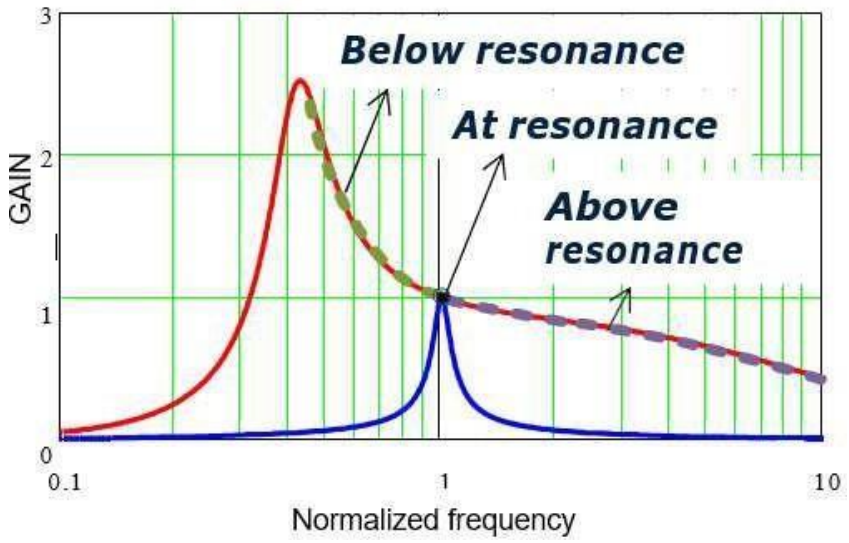

Fig. 2.9 Gain vs Normalized frequency curve

2.5.1 At Resonant frequency:

In this mode Switching frequency became equal to the series resonant frequency i.e fs = fr. In positive switching voltage Switches S1 and S4 are ON. At every half switching cycle, the resonant inductor current became equal to the magnetizing current and the rectifier current reaches zero. Gain of the resonant tank will be 1 (unity).

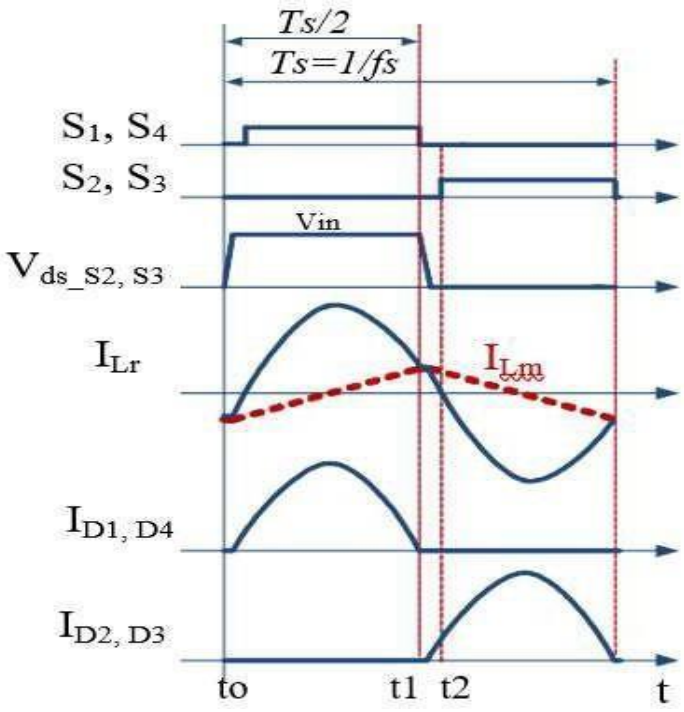

Fig 2.10 At resonant frequency

2.5.2 Below Resonant frequency:

In this mode Switching frequency became less than the series resonant frequency i.e (fs< fr). Even though the magnetizing current is still there in this case, power transmission stops because the resonant current equals the magnetizing current before the driving pulse width is finished. While still accomplishing primary Zero Voltage Switching (ZVS) and permitting secondary soft commutation of the rectifier diodes, it is feasible to run below the series resonant frequency. The secondary-side diodes must work in discontinuous current mode, increasing the current that flows in the resonant circuit, to retain the same energy delivery to the load. Greater conduction losses develop on the main and secondary sides as a result of the enhanced current. In addition, it is vital to keep in mind that basic ZVS may be affected if the switching frequency goes too low. Massive switching losses and other problems may occur from this.

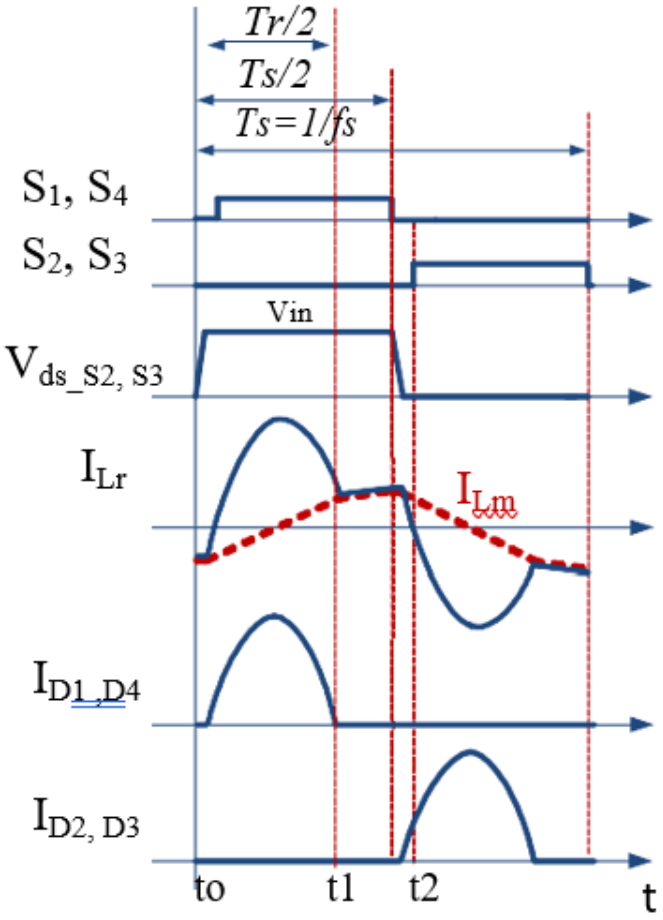

Fig 2.11 Below Resonant frequency

2.5.3 Above Resonant frequency:

In this mode Switching frequency became more than the series resonant frequency (fs>fr). The primary side of the resonant circuit exhibits a reduced circulating current. This is due to the continuous-current mode of the resonant circuit's current, which leads to a lower RMS current for the same load, resulting in decreased conduction losses. Although there may be reverse recovery losses and the rectifier diodes are not softly commutated, it is still possible to achieve primary Zero Voltage Switching (ZVS) when operating above the resonance frequency.

In light-load conditions, operating above the resonance frequency can lead to significant increases in frequency. The analysis that has come before has demonstrated that the converter may be created by altering f_{sw} on either side of f_0, using $f_{sw} = f_0$ or $f_{sw} > f_0$, or both.

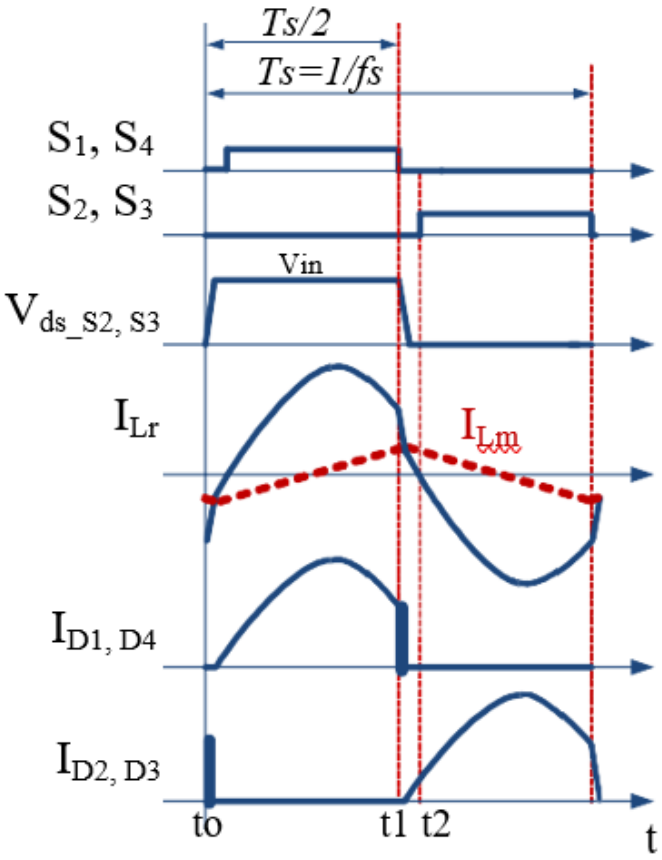

Fig 2.12 Above Resonant frequency

2.6 Comparison between half bridge and full bridge:

LLC Full-bridge converter produce a square wave with no DC offset, and the maximum amplitude will be the input voltage (V_{IN}) Fig 2.13

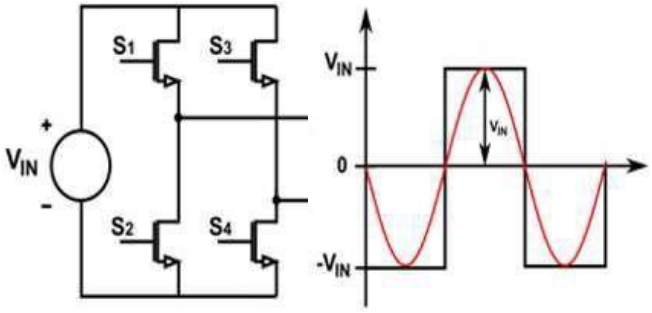

Fig 2.13 Full bridge topology

LLC half bridge converter generates a square wave form with DC offset value $\frac{V_{in}}{2}$

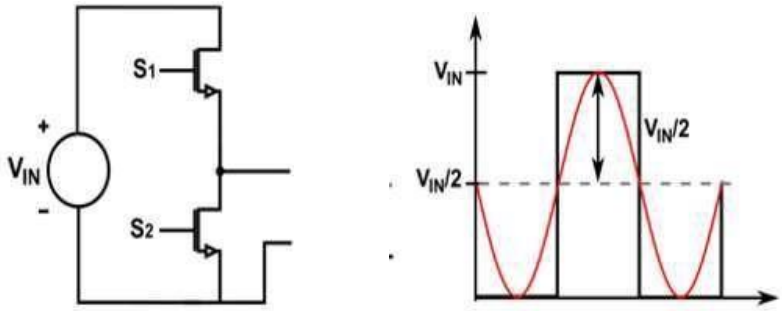

Fig 2.14 Half bridge topology

Primary Bridge - Half-Bridge compared to Full-Bridge						
I_{rms}	I_{rms}^2	Number of FETs	Total FETs conduction losses	N_p	R_{pr}	Transformer primary copper loss
x 2	x 4	÷ 2	x 2	÷ 2	÷ 2	x 2

Table 2.1 Comparison between half and Full bridge at primary

2.7 Comparison between Full-bridge rectifier and full-wave rectifier circuit:

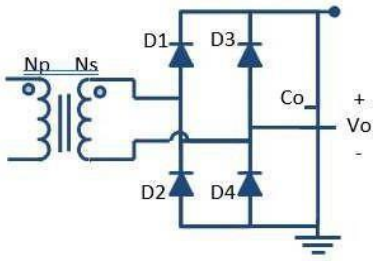

Fig 2.15(a) Full-bridge rectifier

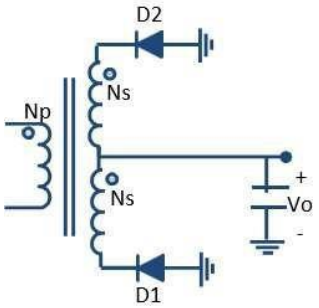

Fig 2.15(b**)** Full-wave rectifier

Secondary Rectifier - Full-Wave compared to Full-Bridge						
Diode voltage rating	Number ofdiodes	Diode conduction losses	Number of secondary windings	R_{sec} per winding	I_{rms} per winding	Transformer secondary copper loss
$\times 2$	$\div 2$	$\div 2$	$\times 2$	$\times 2$	$\times \sqrt{0.5}$	$\times 2$

Table 2.2 Comparison between Full wave and Full bridge at secondary

2.8 Chapter Summary:

In this chapter we have discussed about series, parallel and LLC resonant converter. In detail analysis of Full bridge LLC resonant converter and its operation is discussed in this chapter. We have also studied the different modes of LLC. Comparison between half and full bridge on primary side and Full bridge and full wave rectifier on secondary side is also discussed.

CHAPTER-3
DESIGN OF FULL BRIDGE LLC RESONANT CONVERTER

3.1 Overview

To Design full-bridge LLC resonant converter we need to obtain the Gain or transfer function of system. The Transfer function of this LLC converter is the mathematical relation between input to output voltage gain. To get transfer function in pulse-width-modulated switching converters state space averaging is used. But for LLC converter this method is not successful.

3.2 First harmonic approximation:

For LLC resonant converter we use first harmonic approximation (FHA) method. In first harmonic approximation (FHA) method we ignore the higher order frequency of square wave which we get after power switching and we consider only fundamental frequency waveform.

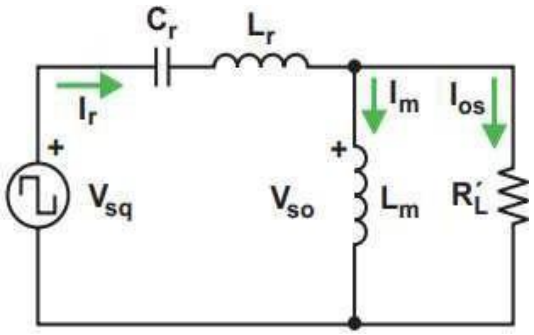

Fig 3.1 Non sinusoidal circuit.

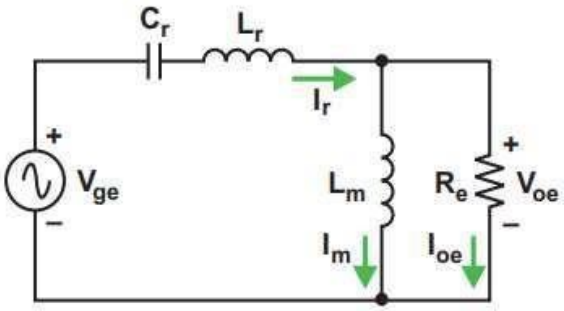

Fig. 3.2 Sinusoidal circuit

In above circuit square voltage (V_{sq}) fig 3.1 and fundamental voltage (V_{ge}) of square voltage (V_{sq}) fig 3.2 is shown

Voltage relation between the square waveform voltage (V_{ge}) and fundamental voltage (V_{sq}) is:

$$V_{1gepk} = \frac{4}{\pi} V_{sq} \qquad (3.1)$$

Where,

V_{1gepk} = peak fundamental voltage

V_{sq} = Square wave voltage

3.3 Equivalent LLC converter:

For calculation of LLC Converter, we have Referred the resistance R_L from secondary side to primary side. On secondary side we have DC voltage whereas on Primary side LLC tank side we have AC voltage. Hence the resistance referred on AC side is R_{ac}. We will derive the voltage, current and resistance on primary side. Also due to transformer turns ratio we have to multiply the referred value with turns ratio (n).

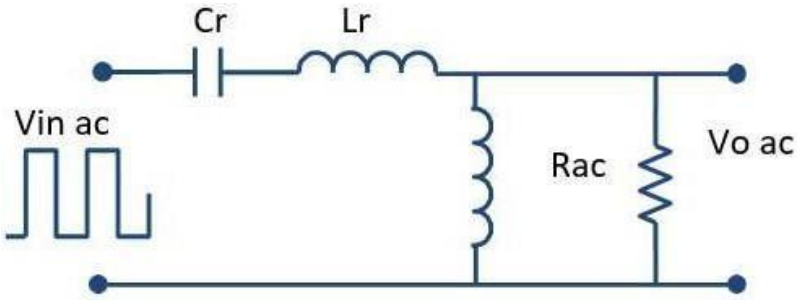

Fig 3.3 Equivalent LLC circuit

RMS voltage at input of LLC tank is:

$$V_{ge} = \frac{2\sqrt{2}}{\pi} V_{sq} \tag{3.2}$$

RMS voltage at output of LLC tank is:

$$V_{ac(rms)} = \frac{2\sqrt{2}}{\pi} * n * V_0 \tag{3.3}$$

RMS current at output of LLC tank is:

$$I_{ac(rms)} = \frac{\pi}{2\sqrt{2}} * \frac{1}{n} * I_0 \tag{3.4}$$

where:

$V_{ac(rms)}$ =Rms voltage at LLC tank output

$I_{ac(rms)}$ = Rms current at LLC tank output

V_0 = Load output voltage

I_0 =Load output current

Equivalent resistance referred at primary side:

To derive equivalent resistance, compare DC power at load side with AC power at tank side.

$$P_{DC} = P_{AC}$$

$$I_0^2 R_L = I_{ac}^2 R_{ac}$$

$$R_{ac} = \frac{8 * n^2 * V_0^2}{\pi^2 * P_0} \qquad (3.5)$$

Where:

R_{ac} = resistance referred to primary side

P_0 = Output power

V_0 = Output voltage

n= Turns ratio of transform

3.4 Design Specification:

Parameters	Values
Input voltage range (Vdc_min - Vdc_max) Nominal voltage (Vdc_nom)	(360 – 420) V 400 V
Output voltage range (Vo_min – Vo_max)	(35 – 58) V
Output current range (Io)	(1- 55) A
Output power (Po)	3.3 KW
Equivalent resistance	61.42 Ω
Turns ratio (n)	8:1
Resonant Inductor	26 µH
Magnetising Inductor	106 µH
Resonant capacitor	43.2 nF
Quality factor	0.4
Inductance ratio	4
Resonant frequency	105kHz
Switching frequency	(105-255)kHz

Table 3.1 Design specification value

We are designing our LLC converter for 3.3KW load. 230V AC supply is given from grid, after rectification and boost PFC we get 400V DC at our Full bridge LLC converter switches. Input voltage at LLC converter switches range from (360-420) V DC (Nominal voltage of 400V DC).

Output Voltage range at Load is range from (33-58) V DC. Output Current range at Load is range from (1-55) A.

Turns ratio of transformer is 8:1. Switching frequency of LLC ranges from (105-255) kHZ and resonating frequency is 105kHZ. We will get best system response when switching frequency is near to resonating frequency. Normalized frequency is calculated by ratio of Switching frequency to resonating frequency. After calculation we get maximum and minimum normalized frequency range also maximum and minimum Gain range.

Gain vs Normalized frequency curve is drawn at different Quality factor and Inductance ratio. At a particular Quality factor and inductance ratio, which curve gets fitted in the range of maximum and minimum gain, that value of Q and m gets selected.

Selection of Q & m and Switching frequency are shown in Calculation part.

3.5 Design flow graph:

To Design our LLC full bridge converter, we will follow the following procedures.

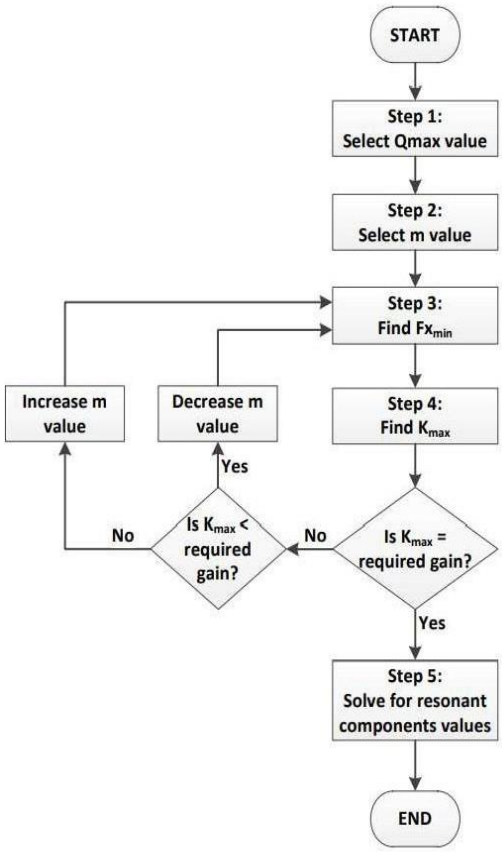

Fig 3.4 Design flow chart of LLC resonant converter

3.6 Selecting the Switching frequency:

Usually, the switching frequency range near or below the 150kHZ because EMI conduction testing starts from 150kHZ. For unique application we required different frequency ranges. The converter's size increases as the switching frequency decreases, making switching losses and ZVS efficiency less significant. When conduction losses become the main factor, the LLC converter becomes less appealing. If the switching frequency is increased then the advantages of the LLC converter are more when compared to hard-switched converters.

For too high frequency then some other factor like cost, switching loses and magnetic core losses became concern.

So, according to our application we select switching frequency.

3.7 Procedure of Selecting Q and m:

For Selecting Quality factor (Q) and inductance ratio (m) we have to draw the graph between Gain (M_g) and Normalised frequency (f_n) at different Q and m.

If switching frequency is same as series resonant frequency the no matter what will be load the gain will always be around 1. In this case frequency variation is very narrow and input voltage became equal to output voltage.

3.7.1 Selecting Q value:

For fix m, if we increase the value of Q then our gain curve will narrow down towards series resonant frequency and if we decrease the value of Q then our gain curve will spread out towards parallel resonant frequency. Increasing the quality factor means decreasing the load. So if we change our load from infinity to 0 then our frequency curve will moves from parallel resonant frequency to series resonant frequency (f_0).

We select that value of Q and m for which our gain comes under the range of maximum and minimum gain value.

$$M_{g\_\min} \leq M_g \leq M_{g\_\max}$$

As we know LLC resonant converter works under inductive region, So quality factor (Q) should be less than $Q_{\max}$ so that our operation does not enter Capacitive region.

3.7.2 Selecting m value:

For fix Q, smaller m makes the gain curve more peak. Smaller inductance ratio (m) means larger resonant inductance (L_r) and small magnetising inductance (L_m) which helps the ZVS. A smaller quality factor (Q) makes higher peak gain and larger quality factor (Q) makes smaller peak gain. So, we have to select the value of quality factor (Q) accordingly.

At Low m value:

I. Gain curve has higher peak
II. Frequency modulation curve is narrow
III. Having more Control and regulation

At High m value:

I. Magnetizing inductance will be high.
II. Magnetizing circulating current will be lower
III. Have high frequency.

Fig 3.5 shows Gain vs Normalized frequency curve at different quality (Q) factor by keeping the inductance ratio (m) = 4.

So, from above curve at Q = 0.4 and m = 4, we are getting our desired curve. By selecting above value, we can calculate Resonant tank parameters, Gain and other values.

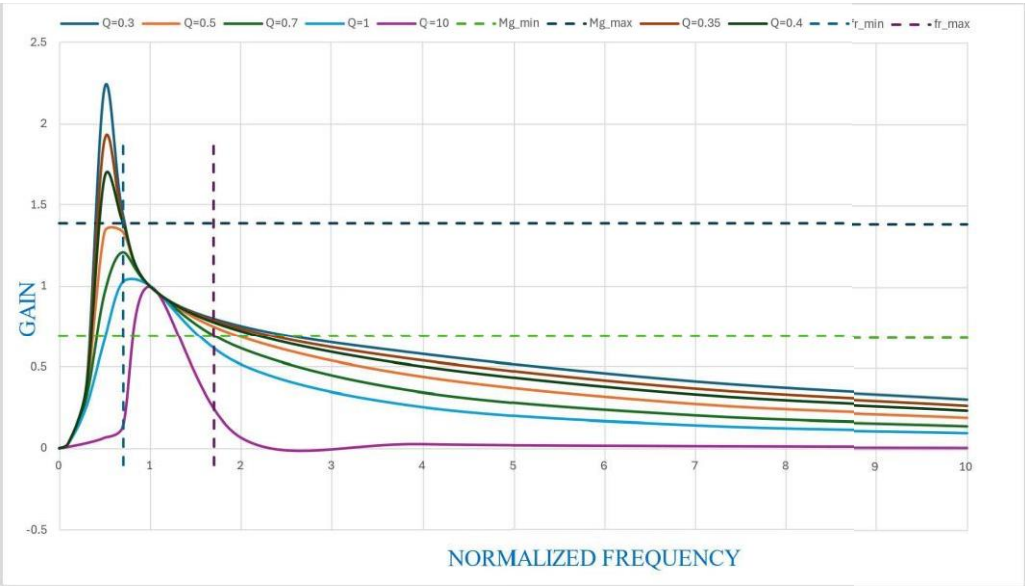

Fig 3.5 Gain (M_g) vs Normalized frequency (f_n) curve

The gain of the LLC resonant converter is:

$$M_g = \frac{V_{o\_ac}}{V_{in\_ac}} = \frac{F_n^2 (m\_1)}{\sqrt{(m * F_n^2 - 1)^2 + F_n^2 (F_n^2 - 1)^2 * (m-1)^2 * Q^2}} \quad (3.6)$$

Where:

M_g = Gain of converter

F_n = Normalized frequency

m = Inductance ratio

Q = Quality factor

3.8 Calculation:

Turns ratio of transformer (n):

$$n = M_g * \frac{V_{in\_nom}}{V_{o\_nom}} = \frac{400}{48} = 8.33 \quad (3.7)$$

Maximum and Minimum gain of converter:

$$M_{g\_\min} = n * \frac{V_{o\_\min}}{V_{in\_\max}} = 8.33 * \frac{35}{420} = 0.694 \quad (3.8)$$

$$M_{g\_\max} = n * \frac{V_{o\_\max}}{V_{in\_\min}} = 8.33 * \frac{60}{360} = 1.388 \quad (3.9)$$

Equivalent load resistance:

$$R_{ac} = \frac{8}{\pi^2} * n^2 * \frac{V_o^2}{P_o} = \frac{8*8.33^2 * 60^2}{\pi^2 * 3300} = 61.42 \quad (3.10)$$

RMS output voltage:

$$V_{ac} = \frac{2*\sqrt{2}}{\pi} * n * V_o = 450 \text{ V} \quad (3.11)$$

RMS output current:

$$I_{ac} = \frac{\pi}{2*\sqrt{2}} * \frac{1}{n} * I_o = 7.33 \text{ A} \quad (3.12)$$

3.8.1 Resonant circuit parameters:

Resonant capacitor (C_r):

$$C_r = \frac{1}{2*\pi * Q * f_{sw} * R_{ac}}$$

$$= \frac{1}{2*\pi * 0.4 * 150 * 10^3 * 61.42} = 43.2 \text{ nF} \quad (3.13)$$

Resonant inductor (L_r):

$$L_r = \frac{1}{(2*\pi * f_{sw})^2 * C_r}$$

$$= \frac{1}{\left(2*\pi*150*10^3\right)^2 * 43.2*10^{-9}} = 26 \text{ µH} \quad (3.14)$$

Quality factor (Q):

$$Q = \frac{\sqrt{L_r / C_r}}{R_{ac}} = \frac{\sqrt{26*10^{-6} / 43.2*10^{-9}}}{61.42} = 0.4 \quad (3.15)$$

Resonant frequency (f_r):

$$f_r = \frac{1}{2*\pi*\sqrt{L_r * C_r}} = 150 \text{ kHZ} \quad (3.16)$$

Inductance ratio (m):

$$m = \frac{L_m}{L_r} = 4 \quad (3.17)$$

Magnetising Inductance (L_m):

$$L_m = m * L_r = 4*26*10^{-6} = 104 \, \mu\text{H} \quad (3.18)$$

Dead time between MOSFETs for ZVS:

$$\tau_{dead} \geq 16 \times C_{eq} \times f_{sw} \times L_m \approx 140\text{ns} \quad (3.19)$$

3.9 Magnetic design:

When developing an LLC resonant converter for any application, magnetic design is a crucial necessity. An important obstacle in magnetic design is the careful selection of the necessary core material and the wire used for winding the transformer. In order to assess the magnetic design, other design approaches can be employed. However, this section focuses on explaining two specific ways: Transformer design based on the area product (AP) and design based on core geometry (Kg). This study assesses magnetic design by analysing the core's geometry.

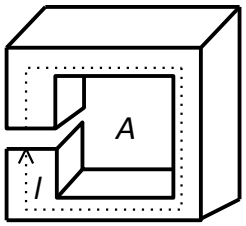

Fig. 3.6 Magnetic core

Voltage across the winding:

$$V = L * \frac{di}{dt} \tag{3.20}$$

$$V = n * \frac{d\phi}{dt} \tag{3.21}$$

From 3.20 and 3.21

$$L * \frac{di}{dt} = n * \frac{d\phi}{dt} \tag{3.22}$$

By integrating both side

$$LI_{pk} = n * A_c * B_{\max} \tag{3.23}$$

After rearranging (4.22), cross-section area of core, Ac can be determined as:

$$A_c = \frac{LI_{pk}}{nB_{\max}} \tag{3.24}$$

The current density will be:

$$J = \frac{I_{rms}}{W_A} \tag{3.25}$$

Winding area Aw:

$$A_{w1} = \frac{n_i W_{Ai}}{k} = \frac{n_i I_{rmsi}}{JK} \qquad (3.26)$$

For primary and secondary side windings total winding area, Aw can be calculated as:

$$A_w = A_{w1} + A_{w2}$$

$$A_w = \frac{n_1}{JK} \sum_i I_{rms} \frac{n_i}{n_1} \qquad (3.27)$$

Product area will be the product of core cross-section area and winding area as:

$$A_p = A_c * A_w = \frac{L_1 I_{pk1} \sum_i I_{rms1} * \frac{n_i}{n_1}}{B_{\max} JK} \qquad (3.28)$$

Skin depth is:

$$\varepsilon = \frac{6.62}{\sqrt{f}} 0.0148 \text{ cm} \qquad (3.29)$$

Wire diameter is determined as:

$$D = 2\varepsilon = 0.0296 \text{ cm} \qquad (3.30)$$

The area of bare wire can be calculated as:

$$A_w = \frac{\pi D_2}{4} = 0.000688 \tag{3.31}$$

Electrical coefficient is calculated as:

$$K_e = 0.145 * f^2 * \Delta B^2 * 10^{-4} = 5800 \tag{3.32}$$

Core geometry can be calculated as:

$$K_g = \frac{P_{in} * D_{\max}}{\alpha_e K} = 9.7 \tag{3.33}$$

Current density can be calculated as:

$$J = \frac{2P * \sqrt{D} * 10^4}{f * A_c * \Delta B * W * k_u} = 2108 A / cm^2 \tag{3.34}$$

Area of primary bare wire can be calculated a:

$$A_{wp(b)} = \frac{I_p}{J} = 0.056 cm^2 \tag{3.35}$$

Area of secondary bare wire can be calculated as:

$$A_{ws(b)} = \frac{I_s}{J} = 0.056 cm^2 \tag{3.36}$$

3.10 Chapter Summary:

In this chapter we have Design Full bridge LLC converter for 3.3KW load. We have also studied Equivalent circuits. We did analysis on First order approximation and its equivalent circuits. In this chapter we discussed about switching frequency and criteria to select it.

We have studied Gain vs normalize frequency curve to select proper Quality factor(Q) and inductance ratio (m). To designed the LLC converter, Magnetic design was also studied.

CHAPTER-4
CONTROL OF FULL BRIDGE LLC RESONANT CONVERTER

4.1 Overview:

In this chapter we will discuss about different control methods of Full bridge LLC resonant converter. Here we discuss control loop and methods through which we can regulate output voltage. For varying load, we have to constantly regulate our DC output voltage and current. In this chapter we will control our converter for Resistive load and DC motor. We can also control Athe charging and discharging of EV battery through LLC converter using dual control loop. For control of Resistive load and DC motor load we are applying voltage control loop.

There are two strategies for converter control pulse frequency modulation (PFM) and phase shifting modulation (PSM). As we know to control conventional converter, we vary duty cycle but for LLC converter we need different approach. For LLC resonant converter we vary the switching frequency. In voltage control of LLC resonant converter, we vary the gate pulse of power switches through varying the frequency.

4.2 Pulse frequency modulation (PFM) control:

PFM control involves adjusting the frequency of the gate driver of power MOSFETs to regulate the output voltage. pulse frequency modulation (PFM) id different from Pulse Width Modulation (PWM) where instead of frequency duty cycle varied.

The switching frequency is modified in response to load conditions and the desired output voltage. By controlling the frequency, the impedance of the resonant tank circuit changes, which will control the power delivered to the load. At resonant frequency the converter can operate at or near to series resonant frequency which will minimizes the losses. At resonance voltage and current are in phase which reduces switching losses and reactive power. For light loads, the switching frequency will increase above the resonant frequency and power transfer will decrease. For heavy loads, the frequency will decrease towards the resonant frequency and power transfer will increase.

PFM helps to maintain ZVS or ZCS conditions across various load and input conditions, which will enhance the efficiency and reduces the EMI in switching waveform.

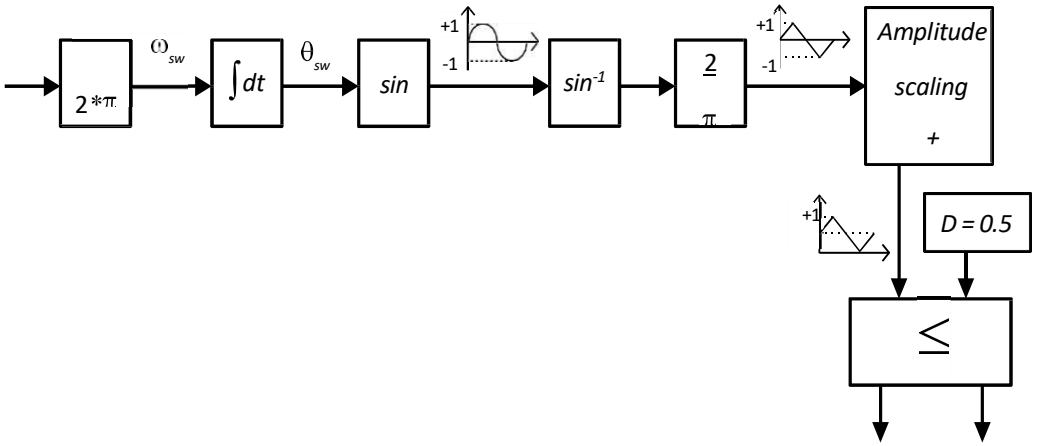

Fig. 4.1 PFM control diagram

The system's input is given the variable frequency f_{sw} which is multiplied by 2π to provide the angular frequency ω_{sw}. After that, this output is sent through an integrator to create θ sw, which is needed to create a sine wave with an amplitude between +1 and -1. Using this, one obtains reference theta by forwarding it to the inverse sine, which is then multiplied by $2/\pi$ to obtain a triangle wave with an amplitude ranging from +1 to -1. This wave is converted into a triangle wave with the same number of cycles but an amplitude range from +1 to 0, with a zero crossing at +0.5, by passing it through circuits for amplitude scaling and clamping. When the created carrier wave's amplitude is less than or equal to 0.5, gate pulses are generated. The carrier wave's duty ratio, which is fixed in the case of PFM, i.e., D=0.5, is compared with the generated wave. To guarantee ZVS during dead time, a time delay is introduced in series with the produced pulses.

4.3 Voltage control of Full bridge LLC resonant converter:

At different loads converter changes its switching frequency to control the power switches for desired voltages. Here in this chapter, we will take resistive loads and Dc motor load to apply voltage control on LLC resonant converter.

In voltage control we firstly senses our output voltage at load and compare that voltage with a reference voltage, an error voltage will generate that error will be given to PI controller to tune our system. In LLC converter PI controller will vary the switching frequency instead of duty cycle to regulates the voltage gain. Pulse frequency modulation will control the switching MOSFETs in according to changing frequency. Switches (Q1, Q4) will on in one cycle and switches (Q2, Q3) will on in other cycle with a proper delay time.

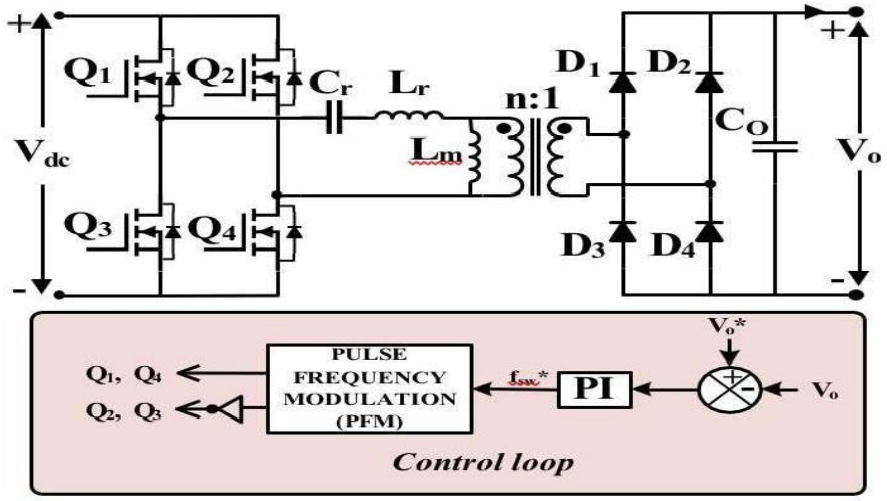

Fig 4.2 voltage control loop

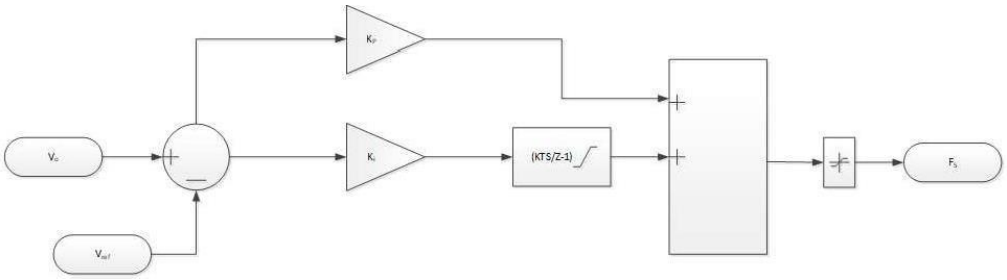

Fig 4.3 PI control loop

4.4 Chapter Summary:

In this chapter we have studied the control strategy of LLC resonant converter. In this chapter we analyse Pulse frequency modulation (PFM) control, and know the reason why we control the LLC through Pulse frequency modulation (PFM) and not use Duty cycle control method. In this chapter we have control the output voltage of Full bridge LLC resonant converter through Voltage control method.

CHAPTER 5
SIMULATION RESULTS

5.1 For Resistive loads:

Fig: 5.1 shows the switching voltage that is fed to Resonant tank circuit. At LLC switches we get 400V dc from boost PFC that 400V switching voltage is given to LLC tank.

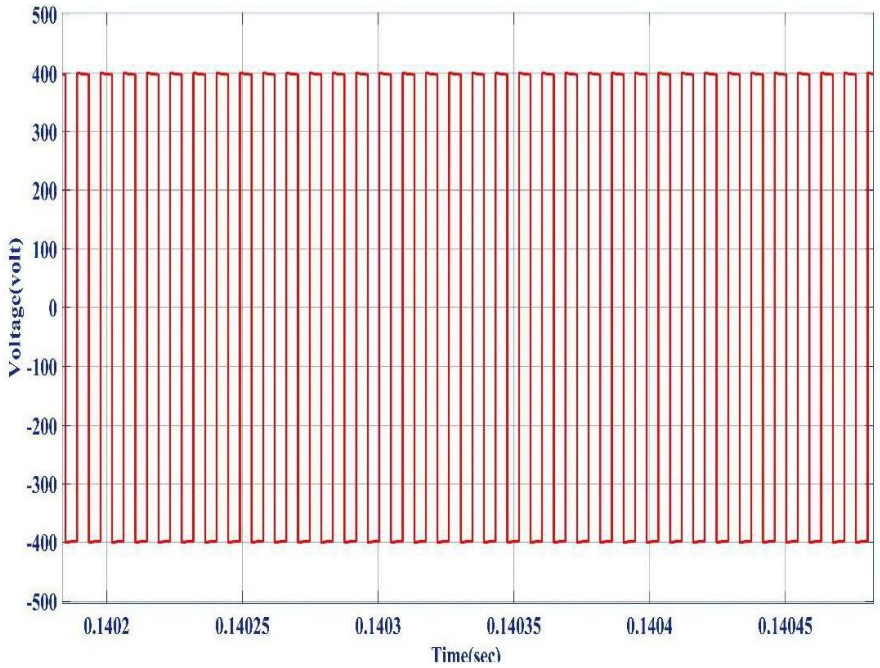

Fig 5.1 Switching voltage at resonant tank

Switches (1 ,4) and switches (2, 3) will be triggered in pair by gate driver with the help of frequency modulation. So, waveform of current and voltage across Switches (1 ,4) will be and switches (2, 3) will be same. Fig 5.2 shows the current and voltage waveform of switch (1 and 4).

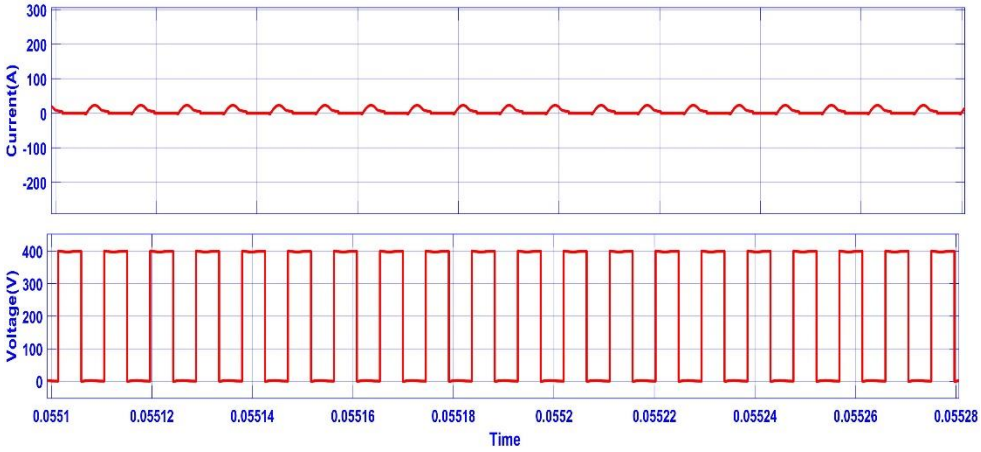

Fig 5.2 current and voltage waveform of when Switches (1, 4) ON

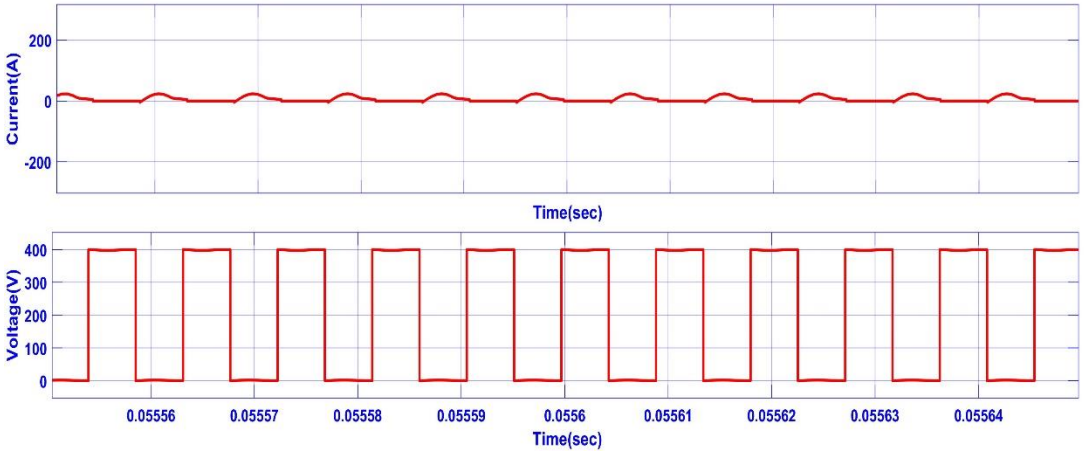

Fig 5.3 current and voltage waveform of when Switches (2,3) ON

Fig5.3 shows the current and voltage waveform across Switches (2, 3) while Switches (S1, S4) are OFF

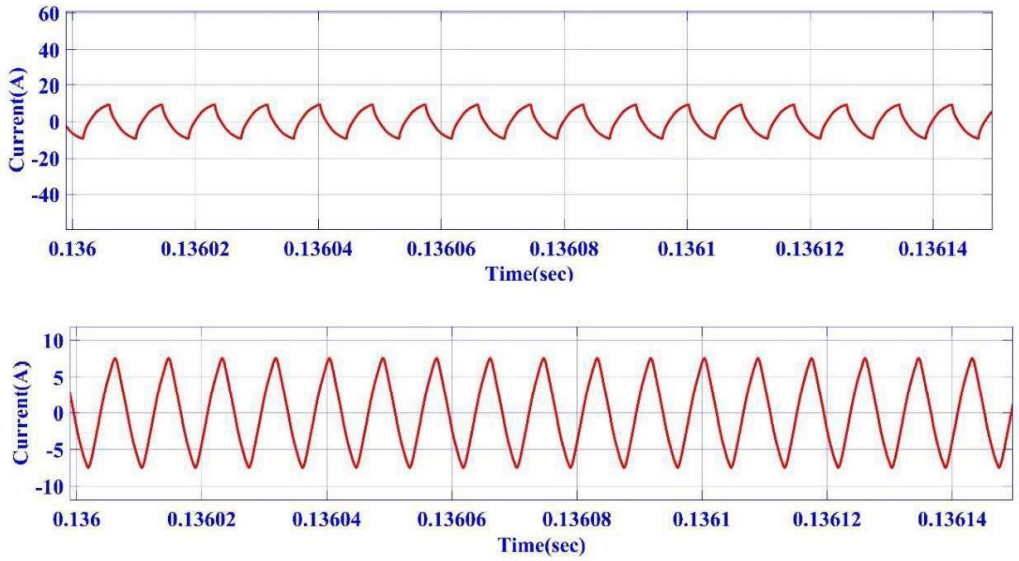

Fig 5.4 Resonant and magnetising Inductor current

Current through Resonant and magnetising inductor shown in fig 5.4. At resonant frequency I_r and I_m crosses each other at the end of half switching cycle. At below resonant frequency I_r reaches before the I_m before completion of half switching cycle. At Above resonant frequency I_r cannot complete its cycle and got interrupted by other half cycle.

Fig 5.5 shows the switching frequency at resistive load. In LLC switching frequency of MOSFETs changes accordingly with the load. At high load switching frequency is less than resonant frequency and Operation can move to capacitive region which is not acceptable. At light load switching frequency is more than the resonant frequency. So we have to choose our operation carefully so that switching frequency should be in region of resonant frequency.

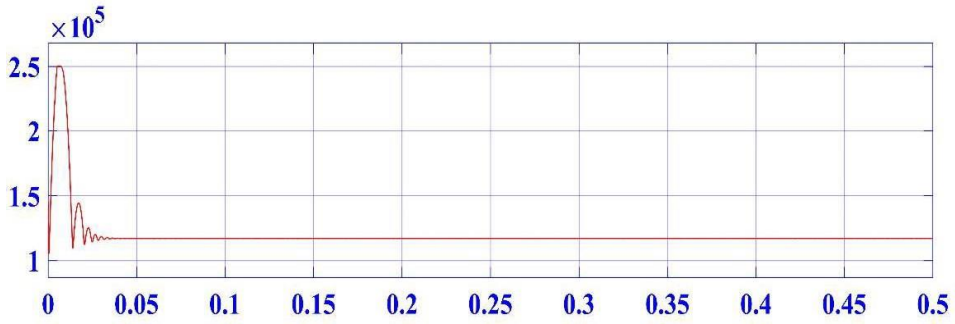

Fig 5.5 Switching frequency

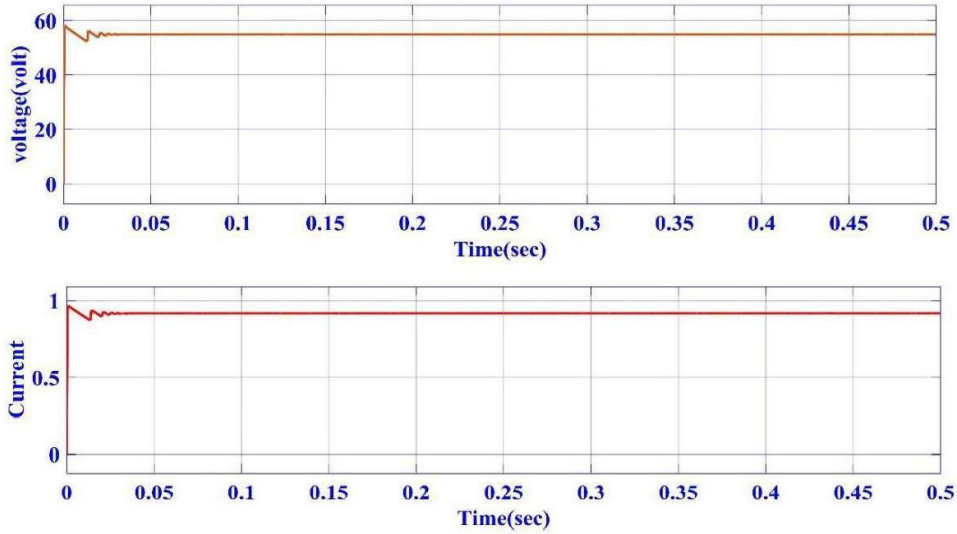

Fig 5.6 Output voltage and current

Output current and voltage shown in fig 5.6. We will get the regulated output voltage and different current of load. If we change the load resistance then switching frequency of our converter will adjust itself to give regulated output voltage.

5.2 For DC motor load:

Here for DC motor load, we will observe the changes in the switching frequency at different torque load. As the torque increases the switching frequency will decreases.

We will also observe the speed of motor, armature current and field winding current of motor at different torque.

At torque τ= 5 nm:

Fig 5.7 shows the frequency response at torque τ= 5 nm

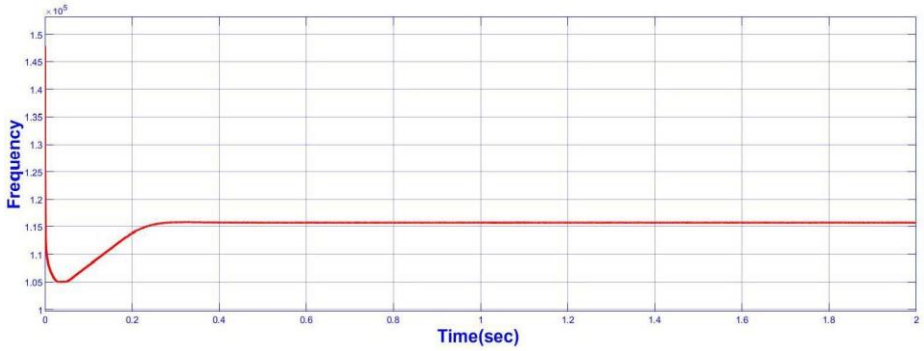

Fig 5.7 Frequency curve

As torque of motor changes, switching frequency of converter will adjust itself to give regulated output. As the torque increases the switching frequency gets reduced and gain curve will narrow down resonating frequency. Similarly, if load at motor gets reduced, switching frequency will increase and gain curve will spread out.

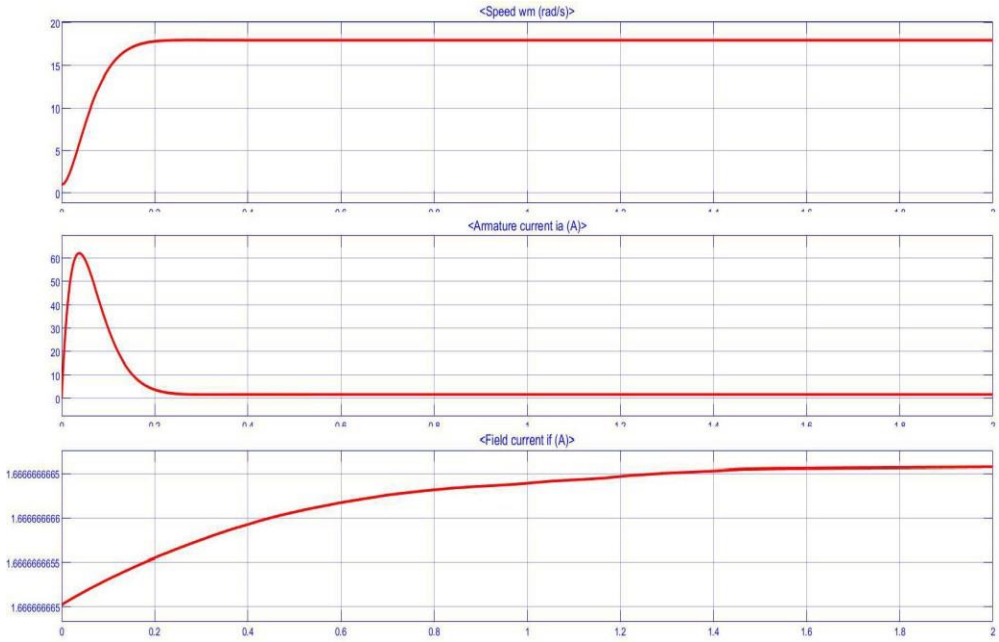

Fig 5.8 speed, armature current, field current curve

Fig 5.8 shows the speed of motor, armature current and field current of the motor at torque τ = 5 nm.

At torque τ = 10 nm:

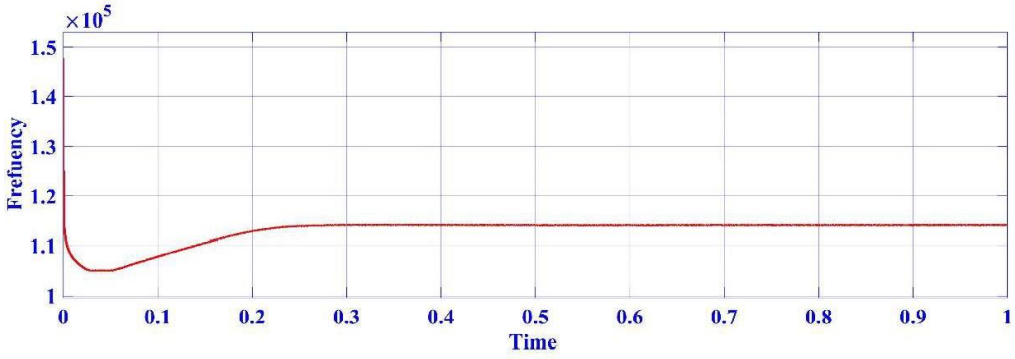

Fig 5.9 frequency curve at τ = 10 nm

From Fig5.9 we can observe that as the load on motor increases from τ = 5 nm torque to τ = 10 nm, the switching frequency of converter decrease. Gain curve will also spread out.

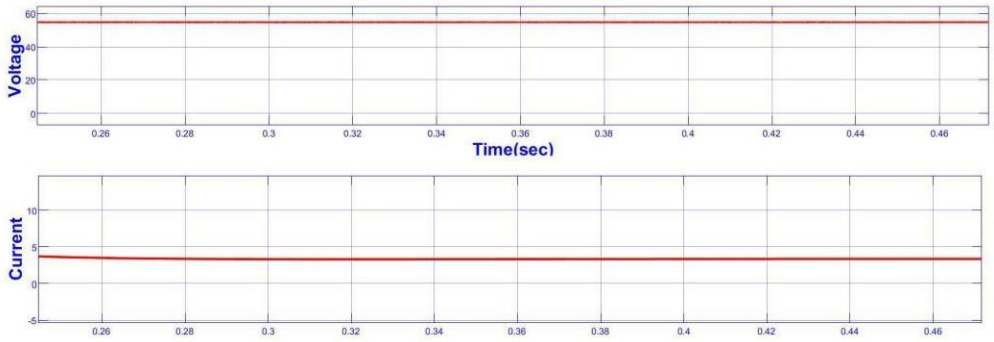

Fig 5.10 Voltage and current waveform

Voltage and Current waveform at τ = 10 nm is shown in Fig 5.10. As torque increases from 5nm to 10nm, current through motor also increase as frequency got updated itself.

5.3 Chapter summary:

In this chapter we have studied the frequency variation to regulate the output voltage at different loads. We have studied how frequency adjust when we increase or decrease the loads. If we increased load, switching frequency will be decreased or vice-versa. In this chapter we have also analyse the voltage and current through load.

CHAPTER-6

CONCLUSION AND FUTURE SCOPE

6.1 CONCLUSION:

In this we have discussed the Resonant converter such as series and parallel resonant converter. To overcome the disadvantages of series and parallel converter, we use combination of series and parallel known as LLC Converter. This study presents an optimisation approach for enhancing the performance of the Full-bridge LLC resonant converter. The procedure focuses on optimising the normalised frequency, fn and a thorough analysis of its effects is conducted. Further, the Pulse frequency modulation (PFM) technique is applied to adjust the frequency of converter in order to accomplish zero voltage switching (ZVS), even in the most not so favourable scenario. The most not so favourable conditions for zero-voltage switching (ZVS) occur when the switching frequency is set to its minimal value and the output current (Io) is set to its maximum value, as previously noted. The resonant tank parameters have been optimised by design optimisation. The operational prototype of the LLC resonant converter has undergone testing with various loads. At output we are using different loads such as resistive and DC load. We analyse the behaviour of frequency at different. At motor load we vary the torque of motor. We record the frequency change at different torque. The acquired results are applicable to the LLC resonant converter as well.

6.2 FUTURE SCOPE:

Subsequent experimental testing will be carried out in order to acquire a more accurate depiction of the overall efficacy of the proposed system. A more robust and efficient controller will be developed for the DC-DC converter to stabilize the dynamic response of the load side. In the future, the commercialization of the Full-Bridge LLC resonant converter prototype will be made possible by the power factor adjustment circuit. We will use the LLC converter for EV charging. A dual control loop will be use for control and EV charging.

REFERENCES

[1] K. Colak, E. Asa and D. Czarkowski, "Dual closed loop control of LLC resonant converter for EV battery charger," 2013 International Conference on Renewable Energy Research and Applications (ICRERA), Madrid, Spain, 2013, pp. 811-815, doi: 10.1109/ICRERA.2013.6749864.

[2] J. -I. Baek, C. -E. Kim, K. -W. Kim, M. -S. Lee and G. -W. Moon, "Dual Half-Bridge LLC Resonant Converter with Hybrid-Secondary-Rectifier (HSR) for Wide-Ouput-Voltage Applications," *2018 International Power Electronics Conference (IPEC-Niigata 2018 -ECCE Asia)*, Niigata, Japan, 2018, pp. 108-113, doi: 10.23919/IPEC.2018.8507956.

[3] S. Sun, J. Fu and L. Wei, "Optimization of High-Efficiency Half-bridge LLC Resonant Converter," *2021 40th Chinese Control Conference (CCC)*, Shanghai, China, 2021, pp. 5922-5926, doi: 10.23919/CCC52363.2021.9550087.

[4] M. D. Dharshinii, K. Pradeepa, S. R. Akshaya and S. Hema, "Open loop and closed loop analysis of LLC resonant converter operating at constant switching frequency by interleaving technique," *2017 International Conference on Information Communication and Embedded Systems (ICICES)*, Chennai, India, 2017, pp. 1-5, doi: 10.1109/ICICES.2017.8070783.

[5] R. R. Boros and I. Bodnár, "LLC Resonant Converter Design and Simulation for PV Motor Drives," *2021 22nd International Carpathian Control Conference (ICCC)*, Velké Karlovice, Czech Republic, 2021, pp. 1-5, doi: 10.1109/ICCC51557.2021.9454640.

[6] G. Jagadan, U. K. Sourav, V. Chathayil, R. S. Kumar and M. V, "Design of LLC Resonant Converter for High Efficiency EV Charging," *2022 IEEE Global Conference on Computing, Power and Communication Technologies (GlobConPT)*, New Delhi, India, 2022, pp. 1-7, doi: 10.1109/GlobConPT57482.2022.9938278.

[7] H. K. T. Tsang, Y. C. Fong, K. L. J. Kan, S. R. Raman and K. W. E. Cheng, "A Study of LLC Converter with Buck Converter for CC-CV Charging," *2020 8th International Conference on Power Electronics Systems and Applications*

[8] S. -Y. Choi and R. -Y. Kim, "Power Loss Analysis of Full-Bridge LLC Resonant Converter," *2021 24th International Conference on Electrical Machines and Systems (ICEMS)*, Gyeongju, Korea, Republic of, 2021, pp. 179-182, doi: 10.23919/ICEMS52562.2021.9634186.

[9] Y. Panov, "Implementation and Stability of Charge Control for Full-Bridge LLC Converter," *2021 IEEE Applied Power Electronics Conference and Exposition (APEC)*, Phoenix, AZ, USA, 2021, pp. 1859-1866, doi: 10.1109/APEC42165.2021.9487256.

[10] F. Zhang, Y. Wang, F. Wang and J. Ming, "Synchronous Rectification Control Strategy for Bidirectional Full-bridge LLC Resonant Converter," *2019 22nd International Conference on Electrical Machines and Systems (ICEMS)*, Harbin, China, 2019, pp. 1-6, doi: 10.1109/ICEMS.2019.8922422.

[11] T. Grigorova and A. Vuchev, "A Study of a Phase-Shifted Full-Bridge LLC Resonant Converter Operating in Continuous Conduction Mode with ZVS," *2022 13th National Conference with International Participation (ELECTRONICA)*, Sofia, Bulgaria, 2022, pp. 1-6, doi: 10.1109/ELECTRONICA55578.2022.9874435.

[12] Y. -C. Huang, Y. -C. Hsieh, Y. -C. Lin, H. -R. Chiu and J. -Y. Lin, "Study and Implementation on Start-Up Control of Full-Bridge LLC Resonant Converter," *2018 IEEE Transportation Electrification Conference and Expo, Asia-Pacific (ITEC Asia-Pacific)*, Bangkok, Thailand, 2018, pp. 1-5, doi: 10.1109/ITEC-AP.2018.8433272.

[13] Y. Wei, Q. Luo and A. Mantooth, "A Hybrid Half-bridge LLC Resonant Converter and Phase Shifted Full-bridge Converter for High Step-up Application," *2020 IEEE Workshop on Wide Bandgap Power Devices and Applications in Asia (WiPDA Asia)*, Suita, Japan, 2020, pp. 1-6, doi: 10.1109/WiPDAAsia49671.2020.9360292.

[14] R. Takarli, M. Adib, A. Vahedi and R. Beiranvand, "A High-Voltage DC-DC LLC Resonant Converter by Using a Symmetrical Voltage Multiplier Circuit," *2023 3rd International Conference on Electrical Machines and Drives (ICEMD)*, Tehran, Iran, Islamic Republic of, 2023, pp. 1-6, doi: 10.1109/ICEMD60816.2023.10429073.

[15] E. Rijanto, A. Nugroho and P. A. Dahono, "A Dynamical Model of Full Bridge LLC Resonant Converter Which Incorporates Power Loss Coefficients for Controller Design," *2018 International Conference on Sustainable Energy Engineering and Application (ICSEEA)*, Tangerang, Indonesia, 2018, pp. 101-105, doi: 10.1109/ICSEEA.2018.8627092.

[16] Shu-huai Zhang, Y. -f. Wang, Bo Chen, Wen-chao Xing and Han Qiu, "An implementation of flexible topology strategy for an interleaved full-bridge LLC resonant converter in residential photovoltaic power systems," *2016 IEEE 8th International Power Electronics and Motion Control Conference (IPEMC-ECCE Asia)*, Hefei, 2016, pp. 3579-3585, doi: 10.1109/IPEMC.2016.7512869.

[17] R. Wang, C. Sun, J. Liu, Y. Huang and Q. Sun, "Large-Signal Modeling for Full-Bridge LLC Resonant Converter Using Extended Hyperbolic Tangent Function," *2022 IEEE International Conference on Energy Internet (ICEI)*, Stavanger, Norway, 2022, pp. 1-6, doi: 10.1109/ICEI57064.2022.00006.

[18] D. Cittanti, M. Gregorio, E. Armando and R. Bojoi, "Digital Multi-Loop Control of an LLC Resonant Converter for Electric Vehicle DC Fast Charging," *2020 IEEE Energy Conversion Congress and Exposition (ECCE)*, Detroit, MI, USA, 2020, pp. 4423-4430, doi: 10.1109/ECCE44975.2020.9236177.

[19] P. P. Gupta, N. Kumar and U. Nangia, "Design and Analysis of LLC Resonant Converter and CCCV Topology for Battery Charging," *2022 2nd Asian Conference on Innovation in Technology (ASIANCON)*, Ravet, India, 2022, pp. 1-5, doi: 10.1109/ASIANCON55314.2022.9909135.

[20] M. Ehsani, K. V. Singh, H. O. Bansal and R. T. Mehrjardi, "State of the Art and Trends

in Electric and Hybrid Electric Vehicles," in *Proceedings of the IEEE*, vol. 109, no.

6,
pp. 967-984, June 2021, doi: 10.1109/JPROC.2021.3072788.

[21] S. Shafiee, M. Fotuhi-Firuzabad and M. Rastegar, "Investigating the Impacts of Plug- in Hybrid Electric Vehicles on Power Distribution Systems," in *IEEE Transactions on*
Smart Grid, vol. 4, no. 3, pp. 1351-1360, Sept. 2013, doi: 10.1109/TSG.2013.2251483.

[22] A. Ahmad, Z. Qin, T. Wijekoon and P. Bauer, "An Overview on Medium Voltage Grid Integration of Ultra-Fast Charging Stations: Current Status and Future Trends," *IEEE*
Open Journal of the Industrial Electronics Society, vol. 3, pp. 420-447, 2022.

[23] G. Rituraj, G. R. C. Mouli and P. Bauer, "A Comprehensive Review on Off-Grid and
Hybrid Charging Systems for Electric Vehicles," *IEEE Open Journal of the Industrial Electronics Society,* vol. 3, pp. 203-222, 2022.

[24] J. Prakash and I. Sarkar, "Comparison of PFC Converter Topology for Electric Vehicle Battery Charger Application," *2022 IEEE Students Conference on Engineering and Systems (SCES)*,Prayagraj, India, 2022, pp. 1-6, 10.1109/SCES55490.2022.9887746.

[25] I. L. Spano, A. Mocci, A. Serpi, I. Marongiu and G. Gatto, "Performance and EMC analysis of an interleaved PFC boost converter topology," *2014 49th International Universities Power Engineering Conference (UPEC)*, Cluj-Napoca, Romania, 2014,
pp. 1-6, doi: 10.1109/UPEC.2014.6934721.

[26] S. S. Sayed and A. M. Massoud, "Review on State-of-the-Art Unidirectional Non- Isolated Power Factor Correction Converters for Short-/Long-Distance Electric Vehicles," in *IEEE Access*, vol. 10, pp. 11308-11340, 2022, doi:
10.1109/ACCESS.2022.3146410.

[27] F. Musavi, M. Edington, W. Eberle and W. G. Dunford, "Evaluation and efficiency
comparison of front end AC-DC plug-in hybrid charger topologies", *IEEE Trans.*

Smart Grid, vol. 3, no. 1, pp. 413-421, Mar. 2012.

[28] D. S. Gautam, F. Musavi, M. Edington, W. Eberle and W. G. Dunford, "An automotive onboard 3.3-kW battery charger for PHEV application", *IEEE Trans. Veh. Technol.*,
vol. 61, no. 8, pp. 3466-3474, Oct. 2012.

[29] B. Lu, R. Brown and M. Soldano, "Bridgeless PFC implementation using one cycle control technique", *Proc. 20th Annu. IEEE Appl. Power Electron. Conf. Expo.*, vol. 2, pp. 812-817, Mar. 2005

[30] F. Musavi, W. Eberle and W. G. Dunford, "A high-performance single-phase bridgeless interleaved PFC converter for plug-in hybrid electric vehicle battery chargers", *IEEE*
Trans. Ind. Appl., vol. 47, no. 4, pp. 1833-1843, Jul./Aug. 2011.

PAPER NAME

CONTENT ONLY.pdf

WORD COUNT	CHARACTER COUNT
7781 Words	**40483 Characters**
PAGE COUNT	FILE SIZE
51 Pages	**3.4MB**
SUBMISSION DATE	REPORT DATE
May 31, 2024 11:53 AM GMT+5:30	**May 31, 2024 11:54 AM GMT+5:30**

- **11% Overall Similarity**

The combined total of all matches, including overlapping sources, for each database.

- 3% Internet database
- 5% Publications database
- Crossref database
- Crossref Posted Content database
- 8% Submitted Works database

- **Excluded from Similarity Report**

- Bibliographic material
- Cited material
- Small Matches (Less then 10 words)